Experimental validation and comparison of a SiC MOSFET based 100 kW 1.2 kV 20 kHz three-phase dual active bridge converter using two vector groups

— **Source link** ↗

Thomas Lagier, Piotr Dworakowski, Cyril Buttay, Philippe Ladoux ...+3 more authors

Institutions: University of Lyon, University of Toulouse, Gdańsk University of Technology

Topics: Galvanic isolation, Three-phase and Transformer

Related papers:

- A single-phase isolated AC-DC converter using an interleaved MMC

- Evaluation of high voltage 15 kV SiC IGBT and 10 kV SiC MOSFET for ZVS and ZCS high power DC -DC converters

- A Dual-Transformer-Based Bidirectional DC–DC Converter of Using Blocking Capacitor for Wide ZVS Range

- Theoretical and experimental analysis of the soft switching process for SiC MOSFETs based Dual Active Bridge converters

- Extended configuration of dual active bridge DC–DC converter with reduced number of switches

Share this paper: ❶ 🐦 in ✉

Experimental validation and comparison of a SiC MOSFET based 100 kW 1.2 kV 20 kHz three-phase dual active bridge converter using two vector groups

Thomas Lagier, Piotr Dworakowski, Cyril Buttay, Philippe Ladoux, Andrzej Wilk, Philippe Camail, Elissa Cresenta Anak Justin

Experimental validation and comparison of a SiC MOSFET based 100 kW 1.2 kV 20 kHz three-phase dual active bridge converter using two vector groups

Thomas LAGIER[1], Piotr DWORAKOWSKI[1], Cyril BUTTAY[1,2], Philippe LADOUX[3], Andrzej WILK[4], Philippe CAMAIL[1,2], Elissa Cresenta ANAK JUSTIN[1]

[1] SUPERGRID INSTITUTE
23 rue Cyprian
69100 Villeurbanne, France
URL: http://www.supergrid-institute.com
[2] Université de Lyon, Laboratoire Ampére, INSA Lyon, CNRS
21 bis avenue Jean Capelle
69100 Villeurbanne, France
URL: http://www.ampere-lab.fr
[3] LAPLACE, UNIVERSITÉ DE TOULOUSE, CNRS, INPT, UPS
2 rue Charles Camichel
31000 Toulouse, France
URL: http://www.laplace.univ-tlse.fr
[4] GDAŃSK UNIVERSITY OF TECHNOLOGY, FACULTY OF ELECTRICAL AND CONTROL ENGINEERING
Gabriela Narutowicza 11/12
80-233 Gdańsk, Poland

Acknowledgements

Keywords

High Voltage power converter, Voltage Source Converter (VSC), MOSFET, Silicon Carbide (SiC), ZVS converters.

Abstract

The Dual Active Bridge appears as a promising DC-DC converter topology when galvanic isolation and bidirectional power flow are required. Among its advantages, Zero Voltage Switching allows the switching losses to be significantly reduced. For high power applications, the three-phase topology variant may be interesting in order to reach a higher power density, especially when a three-phase transformer is implemented instead of three single-phase transformers. Moreover, the transformer vector group offers a new degree of freedom for the designers. In this paper, the authors present the experimental validation of a 1.2 kV – 100 kW – 20 kHz three-phase Dual Active Bridge converter using two medium frequency transformers and different vector groups.

Introduction

The Dual Active Bridge (DAB) topology is an interesting candidate for high power DC-DC converters when galvanic isolation and bidirectional power flow are required. In addition to its modularity and simplicity, Zero Voltage Switching (ZVS) operation allows a higher switching frequency, which in turn enables a higher power density. Compared to the single-phase DAB, the three-phase topology variant, depicted in Fig. 1, allows reducing the input and output filters and transformer size [1–6].

Moreover, since several vector groups (Yy, ΔΔ and even YΔ) can be chosen for the three-phase transformer, a new degree of freedom can be used to optimize the design. Some papers have already studied the three-phase DAB, but the use of a single three-phase medium frequency transformer (instead of three single-phase transformers) is not well documented. Moreover, in this paper, the authors propose a global comparison between two Medium Frequency Transformers (MFT) with two vector groups (Yy and ΔΔ).

After a short introduction of the topology and the DC-DC converter prototype, this paper compares the performance of the transformers and the voltage source inverters (VSI). Then, the performances are summarized in order to identify the configuration which presents the best compromise for this application.
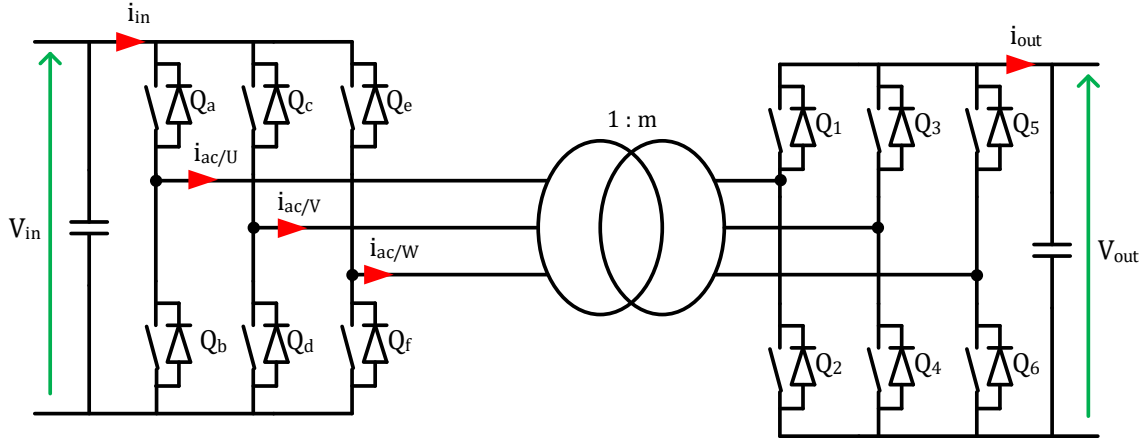
Fig. 1. Three-phase dual active bridge converter

Three phase dual active bridge converter

The three-phase DAB is composed of two VSIs and a MFT. The theoretical analysis of the circuit [2] allows the calculation of the expressions for the transmitted power and the ZVS operating range as a function of the input voltage (V_{in}), the reactance of leakage inductance seen from the primary side of the transformer (X_l) and the ratio between the input and output voltages, calculated by (1)

$$k = \frac{V_{out}}{mV_{in}} \tag{1}$$

where m is the transformer's turns ratio.

Fig. 2 compares the theoretical RMS currents in the switches and the ZVS operating limits for Yy and ΔΔ vector groups.
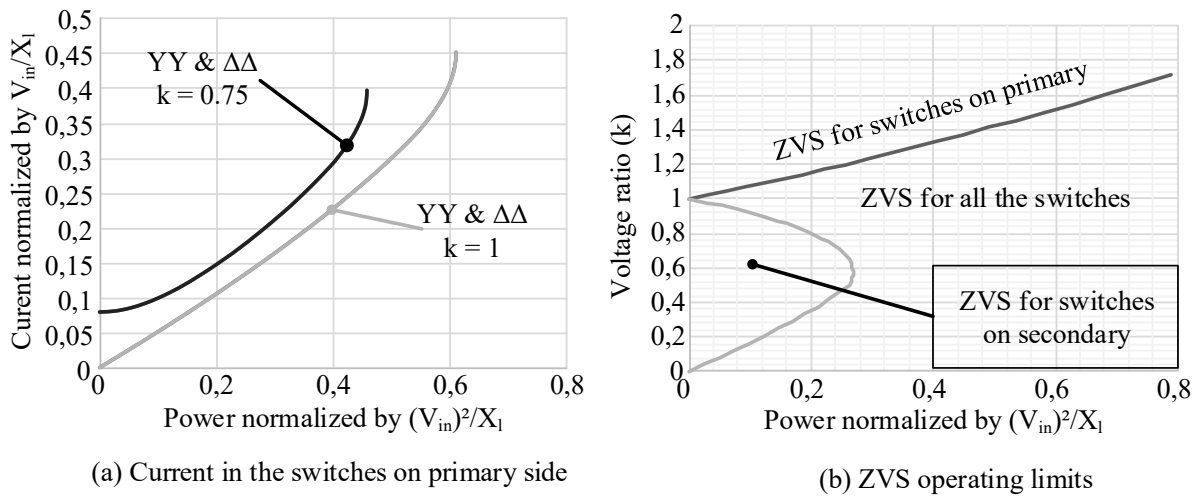
(a) Current in the switches on primary side

(b) ZVS operating limits

Fig. 2. Theoretical current in the switches and ZVS operating ranges for Yy and ΔΔ vector groups calculated using the equations of [2].

As it can be seen, there is no difference between the two solutions. Consequently, the performances and losses of the power switches are expected to be similar.

Experimental validation

Two three-phase MFT prototypes have been developed in order to perform a comparative analysis. For the first prototype T1, the vector group can be changed between Yy and $\Delta\Delta$ while the Yy vector group has been selected for the second prototype T2. Both transformer prototypes were built using MnZn ferrite 3C90 and Litz wire. The design details are presented in [7], [8]. The main transformer specifications for $k = 1$ are presented in Table 1. The core power loss calculation is based on [9], [10] and the winding power loss is based on [11], [12].

Table 1. Three-phase medium frequency transformer specifications at k = 1: MFT T1 (Yy and $\Delta\Delta$) and MFT T2 (Yy only)

	T1 $\Delta\Delta$	T1 Yy	T2 Yy
Winding voltage (V)	980	566	566
Winding current (A)	36	65	65
Core flux density (T)	0.22	0.15	0.27
Winding current density (A/mm^2)	1.2	2.1	2.1
Core power loss at 100°C (W)	432	122	230
Winding power loss at 80°C (W)	155	229	214
Equivalent series resistance (mΩ)	13.7	18.1	17.1
Equivalent magnetizing inductance (mH)	0.2 ... 0.7	0.5 ... 2	1 ... 2.5
Equivalent leakage inductance (µH)	11.3	34	15.8
Dimensions (cm)	67 x 20 x 35		45 x 20 x 30
Weight (kg)	57		36

Even if the theoretical studies have shown similar performances for the two configurations, experimental validations were necessary to validate and compare the behavior of the converter. In order to investigate this, a Silicon Carbide (SiC) based 1.2 kV – 100 kW – 20 kHz DC-DC converter prototype was developed and presented in [1]. The three-phase DAB test bench implementation is presented in Fig. 3.
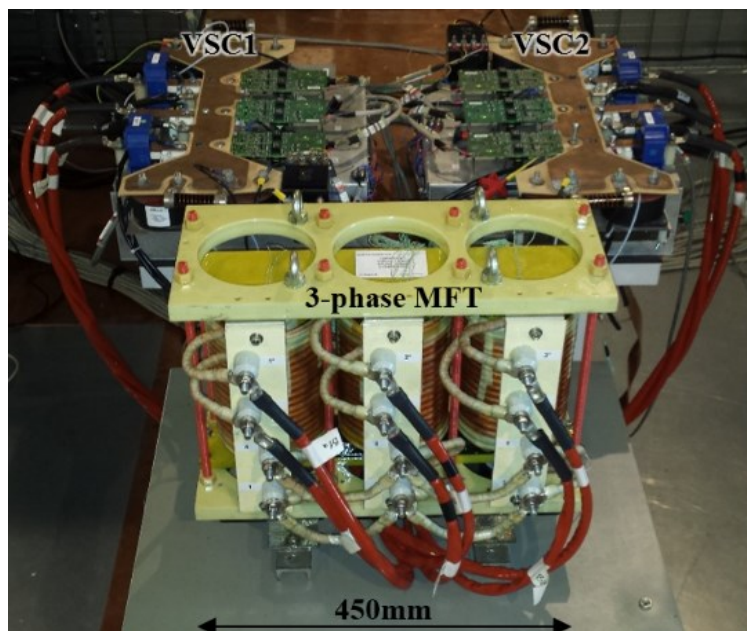
Fig. 3. Three-phase DAB test bench implementation (T2 MFT)

The power circuit is arranged in back-to-back fashion in order to test the DC-DC converter at full power with a minimum energy consumption. The converter output is connected to its input and the whole is supplied from the DC power supply which sets the voltage reference and compensates for the power losses in the converter.

Fig. 4 presents the experimental waveforms for Yy and ΔΔ vector groups, obtained with the MFT T1 prototype.

(a) Yy

(b)ΔΔ

Fig. 4. Experimental waveforms showing the voltages and currents across the windings of the transformer (V_{in} = 1 kV and P_{dc} = 80 kW)

Fig. 5 presents the measured efficiency for all the configurations.

Fig. 5. Measured efficiency for the three configurations at V_{in} = 1.2 kV and k = 1.

As it can be seen, the Yy vector groups present the best efficiency over the entire power range. The following sections explain this difference.

Study of the power losses in the transformer
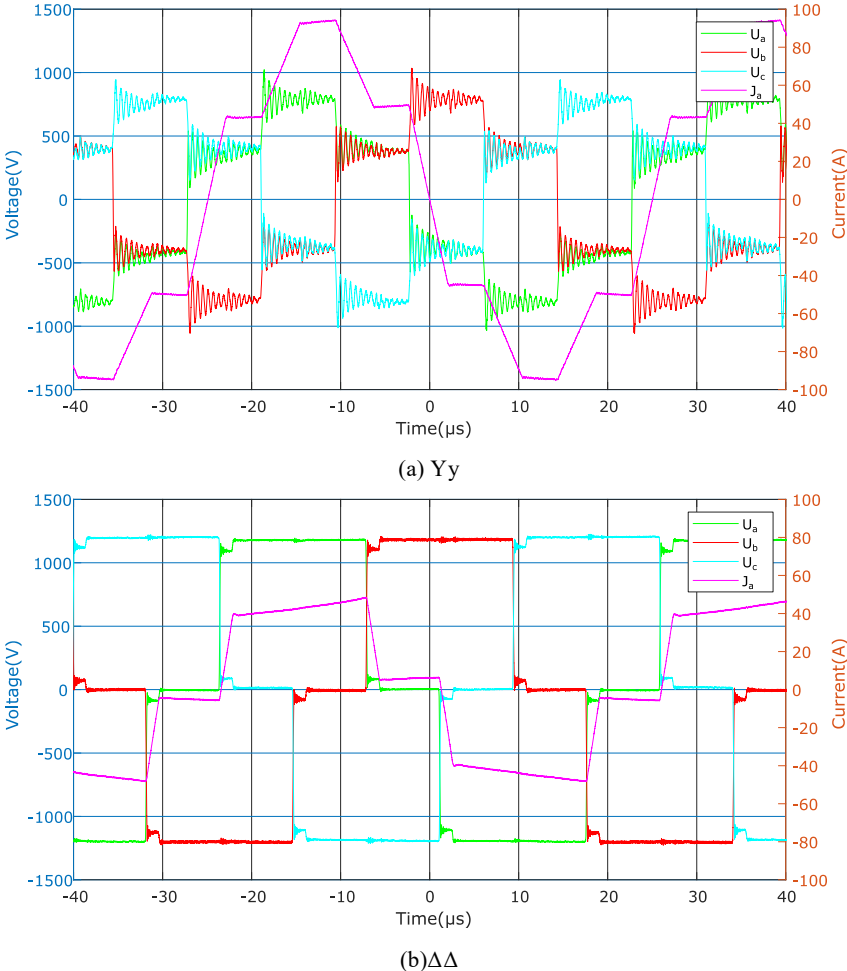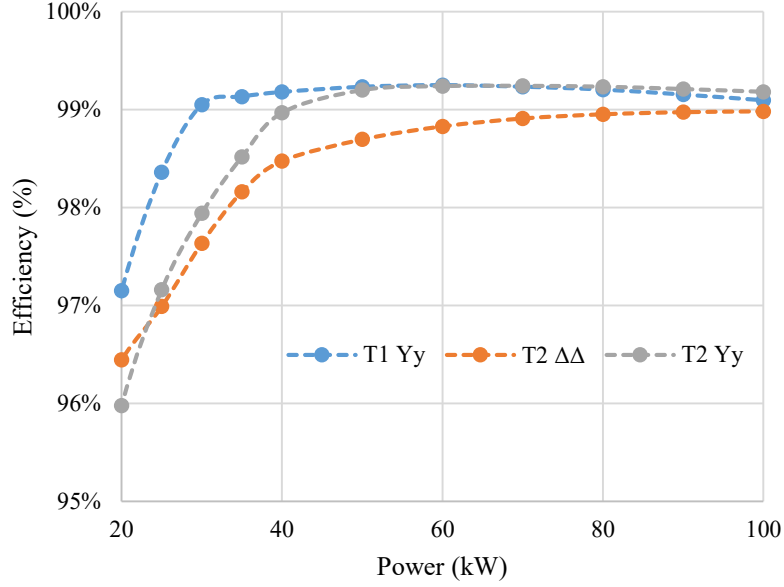
Fig. 6 presents the RMS current values in the windings on the primary side of the transformer. The currents are similar on the secondary side.
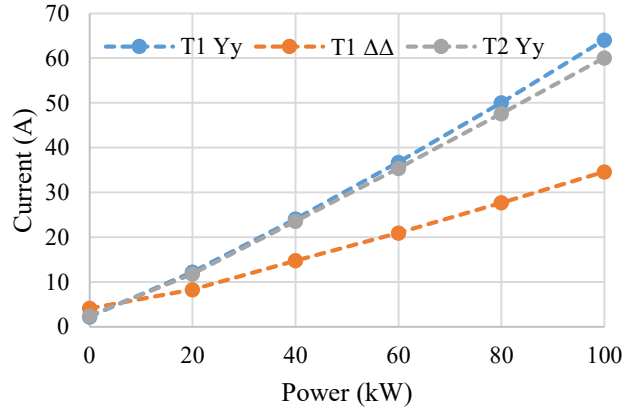
Fig. 6. Comparison of the RMS currents in the transformer primary winding

As expected, the currents in the windings are lower for the ΔΔ configuration, except at low power, where the contribution of the transformer magnetizing current is higher. This causes higher copper losses with ΔΔ configuration for a power lower than 7 kW.

At high power, the ΔΔ currents are lower by a factor of about $\sqrt{3}$. Consequently, at nominal power, the copper losses (RI_{ac}^2) are expected to be smaller, by a ratio of 3 $\left(\left(\sqrt{3}\right)^2\right)$.

Regarding the core losses, the Improved General Steinmetz equation (2-4) [10] can be used to understand their evolution. These losses depend on the voltage across the i-th winding (u_i where i = 1…6), the maximum flux density (B_{max}), the core volume (V_c), the core cross-section (A_c), the frequency (f_{ac}) and the temperature (T). The coefficients used in the equations are depicted in Table 2. With the ΔΔ vector group, the voltage applied on the windings is $\sqrt{3}$ higher than with Yy. However, the maximum flux density is less than $\sqrt{3}$ higher (Table 1). Considering the same transformer design for ΔΔ and Yy,

the core losses are obviously higher with ΔΔ. However, if there were two independent designs, one for ΔΔ and one for Yy, then core losses would be lower with ΔΔ.

Table 2. Ferrite 3C90 Steinmetz coefficients [13]

Parameter	Value
k	3.2
α	1.46
β	2.75
c_0	2.45
c_1	3.1e-2
c_2	1.65e-4

$$P_c = k_s k_T V_c (2B_{max})^{\beta-\alpha} f_{ac} \int_0^T \left| \frac{u_i}{N_1 A_c} \right|^\alpha dt \tag{2}$$

$$k_s = \frac{k}{2^{\beta+1}\pi^{\alpha-1}\left(0.2761 + \frac{1.7061}{\alpha + 1.354}\right)} \tag{3}$$

$$k_T = c_0 - c_1 T + c_2 T^2 \tag{4}$$

With the ΔΔ vector group, the lower copper losses obtained with the lower currents are not sufficient to compensate the increase in core losses caused by the higher voltage. This is the reason why losses are more important in ΔΔ. Moreover, as the core losses depend only on the voltage, they are expected to be constant with the transmitted power. This would explain why the difference in efficiency reduces when the transmitted power increases.

Study of the power losses in the VSI

Fig. 7 presents the RMS current value in the switches of the primary VSI. The currents are similar on the secondary side.
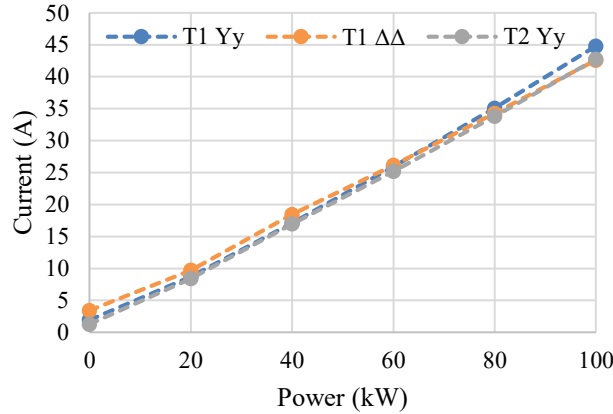
Fig. 7. Comparison of the RMS currents in the switches for the primary VSI (V_{in} = 1.2 kV, k = 1).

It can be seen that the currents are approximately the same for all the configurations. However, for low power (< 60 kW), the higher magnetizing current and higher core losses cause a small increase in the switches current for the ΔΔ vector group. However, the corresponding effect on the conduction losses of the switches is not significant enough to explain the difference in the efficiency.

Regarding the switching losses, a previous study [14] has shown that the soft switching operation depends on the parameters and the configuration of the circuit (leakage inductance, current, voltage). For some conditions, proper soft switching operation might not be obtained, resulting in higher

switching losses. In [14], three cases have been identified as shown in Fig. 8, for the case of our prototype:

1. Case 1: Spontaneous turn-on failure. In this case, the energy stored in the leakage inductance is not important enough to fully discharge the Drain-Source Capacitance (C_{ds}) of the MOSFETs
2. Case 2: Dead time too long. In this case, the energy stored in the leakage inductance is sufficient to discharge the C_{ds} capacitance but because of the freewheeling sequence and the voltage applied by the secondary inverter, the current in the MOSFET cancels before the MOSFET turns-off.
3. Case 3: Soft switching operation. In this case the spontaneous commutation is obtained allowing the reduction of the switching losses.
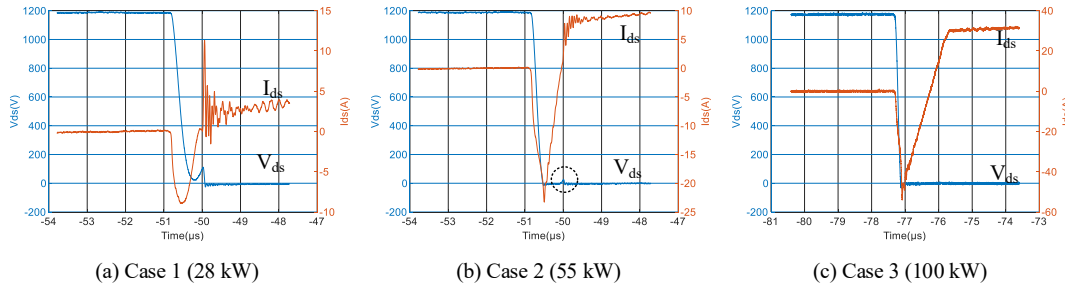

(a) Case 1 (28 kW)   (b) Case 2 (55 kW)   (c) Case 3 (100 kW)

Fig. 8. Switching waveforms for the three cases with the ΔΔ vector group (Vin = 1.2 kV, k = 1). The measured soft switching operating ranges obtained with all the configurations are summarized in Table 3.

Table 3. Soft switching operating range for all configurations (dead time = 500 ns, Vin = 1.2 kV, k = 1)

	T1 ΔΔ	T1 Yy	T2 Yy
Leakage inductance (µH)	11.3	34	15.8
Case 1: Spontaneous turn-on failure	0 → 28 kW	0 → 25 kW	0 → 40 kW
Case 2: Dead time too long	0 → 55 kW	N.A.	N.A.
Case 3: Soft switching operation	55→ 100 kW	25 → 100 kW	40 → 100 kW

As it can be seen, the Yy vector group allows the soft switching operation at lower power.

Fig. 9 depicts the equivalent scheme seen from the inverter's leg on the primary side for the two vector groups before the turn-off of the upper switch. The operation is similar for the other switches.

(a) Yy vector group   (b) ΔΔ vector group

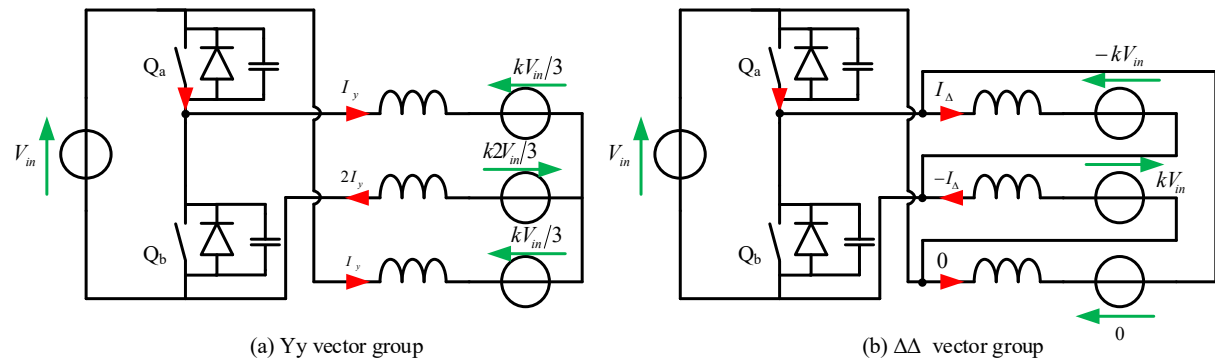Fig. 9. Equivalent scheme of the primary inverter before the turn-off of Qa (phase A) for the two vector groups

As it can be seen, the configuration, voltage and current before the turn-off are different. This explains the differences in the soft switching operating range. Moreover, simplified simulations have confirmed the experimental observations. A complete study, out of the scope of this paper, is nevertheless required

to give more details. However, it clearly appears that the Yy vector group is more favorable to the ZVS operation because of the following reasons:

1. Higher leakage inductance with a higher current in the windings, allowing to get more energy stored in the leakage inductance.
2. Lower voltage applied by the VSI which causes a lower di/dt after the spontaneous commutation of the diodes and a shorter switching duration [14].

Summary

Thanks to the measurement performed and presented in this paper, Table 4 summarizes the observations made in this paper.

Table 4. General comparison of the different vector groups with a single MFT design

	Losses	The most favorable solution
Transformer	Core	Yy
	Windings	ΔΔ
VSI	Switching	Yy
	Conduction	Equivalent

Because of the high switching frequency of the prototype, switching losses have the biggest impact on the efficiency of the converter. It explains why Yy vector group shows the best efficiency.

Conclusion

The three-phase Dual Active Bridge is a promising topology when galvanic insulation and bidirectional power flow are required. Among all the degrees of freedom available for the design of the converter, the transformer vector group can be used to optimize the converter. At first glance, Yy and ΔΔ vector groups can be expected to show similar performance. However, technical aspects experimentally differentiated the two solutions and the Yy configuration showed the best performance.

References

[1]   T. Lagier, L. Chédot, F. W. L. Ghossein, B. Lefebvre, P. Dworakowski, M. Mermet-Guyennet, and C. Buttay, "A 100 kW 1.2 kV 20 kHz DC-DC converter prototype based on the Dual Active Bridge topology," in *2018 IEEE International Conference on Industrial Technology (ICIT)*, 2018, pp. 559–564.

[2]   R. W. A. A. D. Doncker, D. M. Divan, and M. H. Kheraluwala, "A three-phase soft-switched high-power-density DC/DC converter for high-power applications," *IEEE Transactions on Industry Applications*, vol. 27, no. 1, pp. 63–73, Jan. 1991.

[3]   N. Soltau, H. Stagge, R. W. D. Doncker, and O. Apeldoorn, "Development and demonstration of a medium-voltage high-power DC-DC converter for DC distribution systems," in *2014 IEEE 5th International Symposium on Power Electronics for Distributed Generation Systems (PEDG)*, 2014, pp. 1–8.

[4]   Y. Lee, G. Vakil, A. J. Watson, and P. W. Wheeler, "Geometry optimization and characterization of three-phase medium frequency transformer for 10kVA Isolated DC-DC converter," in *2017 IEEE Energy Conversion Congress and Exposition (ECCE)*, 2017, pp. 511–518.

[5]   J. Xue, F. Wang, D. Boroyevich, and Z. Shen, "Single-phase vs. three-phase high density power transformers," in *2010 IEEE Energy Conversion Congress and Exposition*, 2010, pp. 4368–4375.

[6]   A. Garcia-Bediaga, I. Villar, A. Rujas, I. Etxeberria-Otadui, and A. Rufer, "Analytical Models of Multiphase Isolated Medium-Frequency DC–DC Converters," *IEEE Transactions on Power Electronics*, vol. 32, no. 4, pp. 2508–2520, 2017.

[7]   P. Dworakowski, A. Wilk, M. Michna, B. Lefebvre, and T. Lagier, "3-phase medium frequency transformer for a 100kW 1.2kV 20kHz Dual Active Bridge converter," in *2019 45th Annual Conference of the IEEE Industrial Electronics Society (IES)*, 2019.

[8]   P. Dworakowski, A. Wilk, M. Michna, B. Lefebvre, F. Sixdenier, and M. Mermet-Guyennet, "Effective Permeability of Multi Air Gap Ferrite Core 3-Phase Medium Frequency Transformer in Isolated DC-DC Converters," *Energies*, 2020.

[9]   C. P. Steinmetz, "On the Law of Hysteresis," *Transactions of the American Institute of Electrical Engineers*, vol. IX, no. 1, pp. 1–64, Jan. 1892.

[10]   K. Venkatachalam, C. R. Sullivan, T. Abdallah, and H. Tacca, "Accurate prediction of ferrite core loss with nonsinusoidal waveforms using only Steinmetz parameters," in *2002 IEEE Workshop on Computers in Power Electronics, 2002. Proceedings.*, 2002, pp. 36–41.

[11]   P. L. Dowell, "Effects of eddy currents in transformer windings," *Proceedings of the Institution of Electrical Engineers*, vol. 113, no. 8, pp. 1387–1394, Aug. 1966.

[12]   F. Tourkhani and P. Viarouge, "Accurate analytical model of winding losses in round Litz wire windings," *IEEE Transactions on Magnetics*, vol. 37, no. 1, pp. 538–543, Jan. 2001.

[13]   Ferroxcube, "Design of planar power transformers, application note," http://ferroxcube.home.pl/appl/info/plandesi.pdf." .

[14]   T. Lagier and P. Ladoux, "Theoretical and experimental analysis of the soft switching process for SiC MOSFETs based Dual Active Bridge converters," in *2018 International Symposium on Power Electronics, Electrical Drives, Automation and Motion (SPEEDAM)*, 2018, pp. 262–267.